



UNIVERSITY
OF WOLLONGONG
AUSTRALIA

University of Wollongong
Research Online

Faculty of Engineering - Papers (Archive)

Faculty of Engineering and Information Sciences

2012

Terahertz magnetic field induced coherent spin precession in YFeO₃

Runze Zhou
Shanghai University

Zuanming Jin
Shanghai University

Gaofang Li
Shanghai University

Guohong Ma
Shanghai University

Zhenxiang Cheng
University of Wollongong, cheng@uow.edu.au

See next page for additional authors

<http://ro.uow.edu.au/engpapers/5176>

Publication Details

Zhou, R., Jin, Z., Li, G., Ma, G., Cheng, Z. & Wang, X. (2012). Terahertz magnetic field induced coherent spin precession in YFeO₃. *Applied Physics Letters*, 100 (6), 061102-1-061102-4.

Research Online is the open access institutional repository for the University of Wollongong. For further information contact the UOW Library:
research-pubs@uow.edu.au

Authors

Runze Zhou, Zuanming Jin, Gaofang Li, Guohong Ma, Zhenxiang Cheng, and Xiaolin Wang

Terahertz magnetic field induced coherent spin precession in YFeO₃

Runze Zhou, Zuanming Jin, Gaofang Li, Guohong Ma, Zhenxiang Cheng et al.

Citation: *Appl. Phys. Lett.* **100**, 061102 (2012); doi: 10.1063/1.3682082

View online: <http://dx.doi.org/10.1063/1.3682082>

View Table of Contents: <http://apl.aip.org/resource/1/APPLAB/v100/i6>

Published by the [American Institute of Physics](#).

Related Articles

Electrically induced decrease of magnetization in Ca₃Mn₂O₇

Appl. Phys. Lett. **101**, 192407 (2012)

Inducing vortex formation in multilayered circular dots using remanent curves

Appl. Phys. Lett. **101**, 192404 (2012)

Design of remnant magnetization FeCoV films as compact, heatless neutron spin rotators

Appl. Phys. Lett. **101**, 182404 (2012)

Sub-micron mapping of GHz magnetic susceptibility using scanning transmission x-ray microscopy

Appl. Phys. Lett. **101**, 182407 (2012)

Structural, magnetic, and optical properties of Pr and Zr codoped BiFeO₃ multiferroic ceramics

J. Appl. Phys. **112**, 094102 (2012)

Additional information on *Appl. Phys. Lett.*

Journal Homepage: <http://apl.aip.org/>

Journal Information: http://apl.aip.org/about/about_the_journal

Top downloads: http://apl.aip.org/features/most_downloaded

Information for Authors: <http://apl.aip.org/authors>

ADVERTISEMENT



Goodfellow
metals • ceramics • polymers • composites
70,000 products
450 different materials
small quantities fast

www.goodfellowusa.com

Terahertz magnetic field induced coherent spin precession in YFeO_3

Runze Zhou,¹ Zuanming Jin,¹ Gaofang Li,¹ Guohong Ma,^{1,a)} Zhenxiang Cheng,^{2,a)} and Xiaolin Wang²

¹Department of Physics, Shanghai University, 99 Shangda Road, Shanghai 200444, People's Republic of China

²Institute for Superconductor and Electronic Materials, Faculty of Engineering, University of Wollongong, Squires Way, North Wollongong, New South Wales 2500, Australia

(Received 2 December 2011; accepted 15 January 2012; published online 6 February 2012)

We present the magnetic dipole transition at 0.299 THz excited by magnetic component of terahertz electromagnetic pulse in an antiferromagnetic YFeO_3 crystal. The impulsive magnetic field of the terahertz pulse tilts the macroscopic magnetization, causing deviation from the equilibrium position, which is manifested by a sharp absorption at the frequency of the quasiferromagnetic mode of the crystal. The rotating coherent macroscopic magnetization radiates elliptically polarized emission at the frequency of the quasiferromagnetic resonance due to the dichroic absorption in the crystal. © 2012 American Institute of Physics. [doi:10.1063/1.3682082]

Magnetization switching and spin precession in magnetically ordered materials under optical pulses have been investigated extensively in the past decade.^{1–5} On application of visible or near infrared femtosecond pulses to a magnetic structure, a transient magnetic field is generated through the inverse Faraday effect,^{6,7} by which non-thermal magnetization control can be realized with optical pulses.^{8,9} Coherent manipulation of spin precession with ultra-fast laser pulses have been studied extensively in a variety of materials, from ferromagnetic dielectric,^{1,2} and ferromagnetic metal alloys^{4,10} to paramagnetic dielectrics¹¹ and magnetic ionic liquids.¹² It is obvious that the light-matter interaction based on the inverse Faraday effect is an indirect non-linear process. As a result, the interaction efficiency is very low, and a high power laser is needed (amplified femtosecond laser pulses with pulse energy in the microjoule range are used in most studies). On the other hand, the magnetic field of far infrared radiation can be employed to interact with the magnetic dipole of a ferromagnetic structure, and the magnetic interaction efficiency is expected to be greatly enhanced with resonant excitation.

Terahertz time-domain spectroscopy (THz TDS) is a powerful tool for studying the response of materials to electromagnetic (EM) waves, through which information on both amplitude change and phase shift in a material can be obtained.^{13–15} THz spectroscopy has proved to be a very effective method to study the low-energy elementary excitations in solids, such as phonons,¹⁶ excitons,¹⁷ and magnons.¹⁸ In most THz spectroscopy studies, only the electric-field component of the THz radiation is considered to excite electric dipole transitions in the desired materials, and the influence of the magnetic field component of the EM wave is normally neglected. In fact, the magnetic field component of the THz wave plays the dominant role during the interaction process through magnetic dipole transitions in magnetically ordered materials.^{19–21} In this letter, we investigate the magnetic response of a rare-earth orthoferrite, YFeO_3 , crystal by using THz time domain spectroscopy. The interactions

between the electric and magnetic fields of the THz wave with the YFeO_3 crystal are clarified. A sharp absorption at 0.299 THz is observed, which arises from coupling between the impulsive magnetic component of the THz wave and the quasiferromagnetic mode (F-mode) of the YFeO_3 crystal. The subsequent EM wave radiation at the same frequency as the F-mode comes from the free induction decay of the rotation of the macroscopic magnetization.

A *c*-cut yttrium orthoferrite YFeO_3 crystal was grown by the floating zone method. The sample was polished on both sides and has a thickness of 1.33 mm. Below the Néel temperature, $T_N = 645$ K, the YFeO_3 behaves as a canted antiferromagnet with macroscopic magnetization in the direction of the *c*-axis, and the nearest neighbor Fe^{3+} ions are ordered in antiparallel along the *a*-axis of the orthorhombic crystal.²² When a THz pulse is incident along the *c*-axis of the crystal, the magnetic field of the THz pulse can couple with the quasiferromagnetic mode at the frequency of 0.299 THz due to the magnetic dipole transition.²³ At the same time, the electric field of the THz wave can excite both ordinary and extraordinary polarization of the crystal, and birefringence occurs for the incident THz wave.

THz TDS measurements in the transmission configuration were conducted on the *c*-cut YFeO_3 crystal at room temperature in the frequency range of 0.1 to 2 THz. Briefly, the output of a mode-locked Ti:sapphire laser, with pulse duration of 100 fs, centered wavelength of 800 nm, and repetition rate of 80 MHz (Mai Tai HP-1020, Spectra-Physics), was used to generate and detect the THz transient. The emitter and detector of the THz wave were dipole type low-temperature-grown GaAs photoconductive antennas. The polarization of the THz radiation was horizontal, which was parallel to the photoconductive antennas. The polarization of the free induction decay was evaluated by inserting a THz polarizer at polarization angles of $\pm 45^\circ$ with respect to the horizontal direction, respectively.²¹ We have confirmed that the THz waveform obtained from the sum signals between $+45^\circ$ and -45° agrees with the waveform measured directly at the horizontal component.

Figure 1 shows the THz transmission spectra with the electric field of THz wave parallel (a), at 45° (b), and

^{a)}Authors to whom correspondence should be addressed. Electronic addresses: ghma@staff.shu.edu.cn and cheng@uow.edu.au.

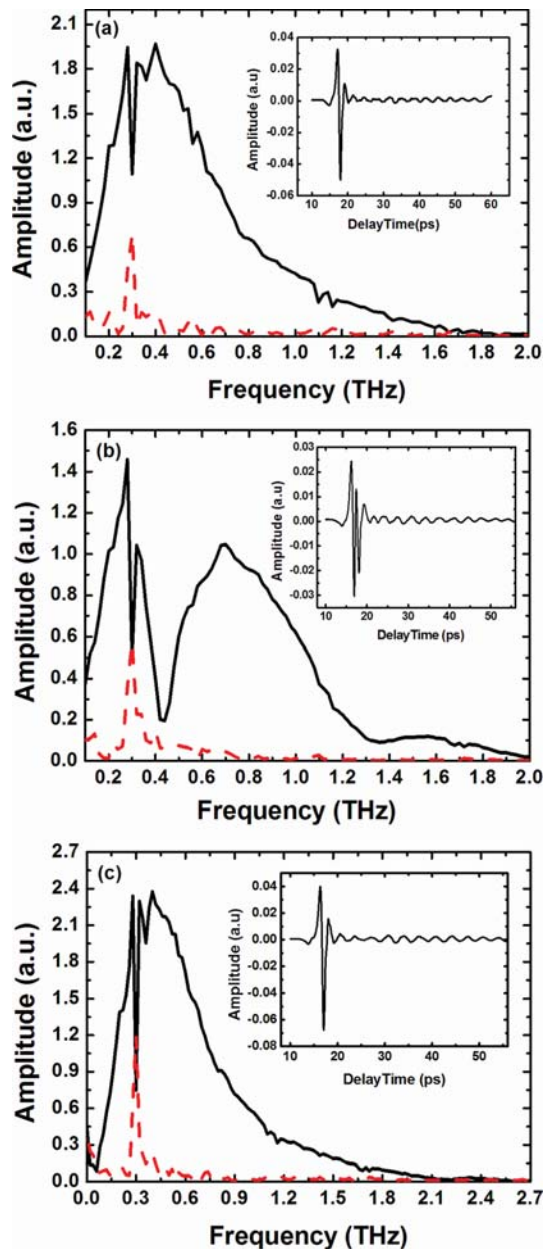


FIG. 1. (Color online) THz transmission spectra of *c*-cut YFeO₃ crystal with the electric field of the THz pulse parallel (a), at 45° (b), and perpendicular (c) to the *a*-axis of the crystal, respectively. The insets show the corresponding transmitted temporal THz pulses. The solid lines in the figure represent the Fourier transform of the corresponding time-domain spectrum (inset) in the time range from 10.5 to 55.5 ps, and the dashed lines show the Fourier transform in the time range from 20.5 to 55.5 ps, respectively.

perpendicular (c) to the *a*-axis of the YFeO₃ crystal. These spectra are obtained from the Fourier transforms of the transmitted temporal waveforms from 10.5 to 55.5 ps (solid lines) and 20.5 to 55.5 ps (dashed lines), as shown in the insets of the figure, respectively. It can be seen that there are two absorption dips. The one at 0.299 THz shows a very narrow band, which does not depend on the polarization of the incident THz wave. The other one, centered around 0.43 THz, strongly depends on the direction of the THz electric-field: the absorption band disappears completely when the electric field is parallel (Fig. 1(a)) or perpendicular (Fig. 1(c)) to the *a*-axis of the crystal, and it becomes most pronounced when

the electric field is set at 45° with respect to the *a*-axis (Fig. 1(b)). The broad high frequency absorption band (0.43 THz) is attributed to the birefringence of the crystal. It is well known that the birefringent refractive indices in the *c*-cut plane of YFeO₃ crystal are $n_a = 4.80$ and $n_b = 4.57$ in the THz frequency range, respectively.²² When the electric field of the incident THz wave is neither parallel nor perpendicular to the *a*-axis of the crystal, the THz waves travel through the crystal in the form of both ordinary and extraordinary waves, and the two THz waves are split in the time domain after they leave the crystal due to the different refractive indices they experience. The dip around 0.43 THz in Fig. 1(b) comes from the birefringent effect of the crystal on the THz wave travelling through it. It can be seen from the inset of Fig. 1(b) that the transmitted THz temporal waveform is shaped by the birefringent effect of the crystal.²³

In this letter, we focus on discussion of the absorption at 0.299 THz, the narrow band absorption shown in Fig. 1, which exhibits no dependence on the polarization of the incident THz wave, indicating that there is neither birefringence nor chirality in the THz range. Here, the absorption can be assigned to the magnetic dipole transition due to the resonant coupling between the magnetic component of the THz wave and the F-mode of the crystal.²⁰ In the excitation of the F-mode, the energy of the impulsive magnetic field is transferred to the spin system instantaneously, diminishing the amplitude of the incident electromagnetic wave. Phenomenally, when the impulsive magnetic field of the THz wave acts on the crystal, the magnetic moment experiences a Zeeman torque (T), which is proportional to the cross product of the magnetic moment (μ) and the impulsive magnetic field (H)

$$T = \gamma \mu \times H, \quad (1)$$

where γ denotes the gyromagnetic constant. As a result, the torque tilts the macroscopic magnetization of the crystal from the equilibrium. It is also noteworthy that the quasi-ferromagnetic resonance for YFeO₃ crystal is around 0.299 THz at room temperature,²⁴ where the resonant mode agrees well with our observations from THz spectra.

The interaction between the impulsive THz magnetic field and the magnetic moment leads to the deviation of magnetization from the equilibrium. After the tipping of the magnetic moment, the tilting magnetic moment starts to precess around an effective magnetic field along the *c*-axis of the crystal. The induced precession of the macroscopic magnetization is expected to emit an EM wave with circular polarization at the same frequency as the absorption, which persists within the transverse relaxation time. In fact, this process is also called free induction decay. The Fourier transform spectra of TDS in the range from 20.5 to 55.5 ps (dashed lines in Fig. 1) come from the new EM radiation due to the free induction decay. It is clearly seen that a peak appears at 0.299 THz, which agrees with the observation of an absorption dip in the figure. It should be mentioned that we did not observe the emission of the quasi-antiferromagnetic mode (AF-mode) at the frequency of 0.53 THz at room temperature,²⁴ and this mode is also not observed from the absorption spectra shown in Fig. 1. The

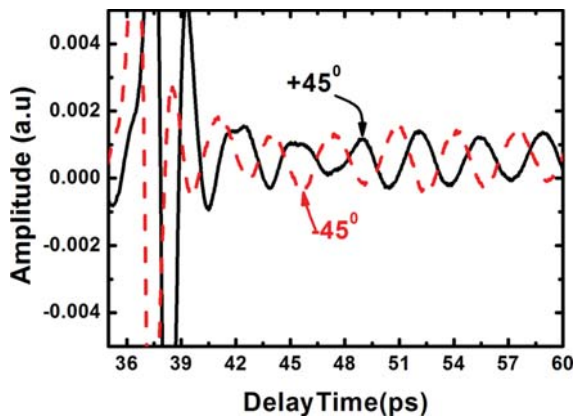


FIG. 2. (Color online) Transmitted THz temporal waveforms with polarizer at $+45^\circ$ (solid) and -45° (dashed) from the horizontal direction, respectively.

broad band absorption appearing at 0.43 THz arises from the birefringence contribution rather than from the AF-mode resonant absorption. This conclusion is also consistent with the THz emission spectrum shown in the figure as well as the observation in the literature.²⁰

In order to study the polarization of the emitted radiation at 0.299 THz, a THz polarizer is inserted before the detector and after the sample, and the polarizer is set to be $+45^\circ$ and -45° to the horizontal, respectively. The measured results are shown in Fig. 2. It should be mentioned that the THz transmission peak in Fig. 2 is time-delayed relative to that in Fig. 1, which is caused by the introduction of polarizer pairs. The oscillation signals at both $+45^\circ$ and -45° originate from the rotating macroscopic magnetization excited by the impulsive THz magnetic field. According to free induction decay, the rotating macroscopic magnetization is expected to radiate a circularly polarized EM emission. However, it is seen from Fig. 2 that the phase shift for the two curves is close to $7\pi/10$, rather than $\pi/2$, which indicate that the generated THz wave has a elliptical polarization instead of circular polarization. The sum and difference of the two spectra give the horizontal and vertical electric field components, respectively.²¹

Figure 3 shows the three-dimensional trajectory plots of the horizontal and vertical components of the THz electric field for the YFeO₃ crystal. It is seen that the THz amplitude in vertical projection (A_V) is larger than that in horizontal projection (A_H), which clearly demonstrates elliptical polarization of the radiation. After tipping with THz pulses, the magnetization rotation around the effective magnetic field is expected to radiate a circularly polarized THz wave. The observed elliptical polarization is believed to come from the dichroic absorption in YFeO₃ crystal.²⁵ In a canted antiferromagnetic structure, the weak ferromagnetism along *c*-axis introduces a symmetry breaking, which leads to a weak absorption dichroism in the crystal. In addition, the damping of the oscillation reflects the relaxation of the magnetization precession, which can be determined from the decay rate of the free induction decay signal. It is found that the free induction decay time is much longer than the measured time window of our set-up, with the lifetime estimated to be longer than 50 ps from the full width at half maximum (FWHM) absorption width given in Fig. 1.

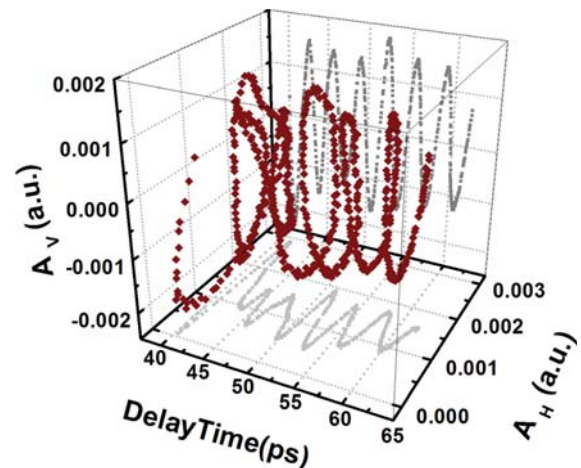


FIG. 3. (Color online) Three-dimensional trajectory plot for the transmitted THz electric field in the YFeO₃ crystal with both horizontal and vertical components: A_H and A_V represent the amplitudes of the horizontal and vertical components, respectively.

Spintronics refers to using the spin of elementary particles to store data and perform processing tasks, in which spin manipulation and coherent control is a key important and challenging task.²⁶ The resonant interaction between ultrashort pulses of magnetic fields and matter provides an effective method to realize the spin manipulation and coherent control.^{19,20,26} The spin precession with long coherence time in antiferromagnetic matter, such as YFeO₃, provides an idea candidate, in which time the spin can be driven and manipulated by external means. On the other hand, the strong and narrow band absorption for F- and AF-mode resonance can be employed to fabricate narrow-band THz band-stop filter and high efficient THz absorber.

In conclusion, the impulsive magnetic component of a THz pulse is used to excite the magnetic dipole transition in YFeO₃ crystal. The sharp absorption at 0.299 THz in the THz spectrum originates from the excitation of the quasiferromagnetic mode of the orthoferrite, and the following EM radiation is demonstrated to arise from the free induction decay, which emits EM radiation at the same frequency as the absorption with elliptical polarization due to the symmetry breaking induced absorption dichroism. Our results demonstrate that magnetic-field component of THz radiation can be employed to investigate the magnetic dipole transition in magnetically ordered materials.

The research is supported by National Natural Science Foundation of China (11174195), Science and Technology Commission of Shanghai municipal (09530501100). Part of work was also supported by National laboratory for infrared physics, Chinese Academy of Science and Shanghai Leading Academic Discipline Project (S30105). Z. X. Cheng thanks the Australian Research Council for support through a future Fellowship.

¹V. Kimel, A. Kirilyuk, A. Tsvetkov, R. V. Pisarev, and Th. Rasing, *Nature* **429**, 850 (2004).

²V. Kimel, A. Kirilyuk, P. A. Usachev, R. V. Pisarev, A. M. Balbashov, and Th. Rasing, *Nature* **435**, 655 (2005).

³V. Kimel, B. A. Ivanov, R. V. Pisarev, P. A. Usachev, A. Kirilyuk, and Th. Rasing, *Nat. Phys.* **5**, 727 (2009).

- ⁴D. Stanciu, F. Hansteen, A. V. Kimel, A. Kirilyuk, A. Tsukamoto, A. Itoh, and Th. Rasing, *Phys. Rev. Lett.* **90**, 047601 (2007).
- ⁵C. Bunce, J. Wu, G. Ju, B. Lu, D. Hinzke, N. Kazantseva, U. Nowak, and R. W. Chantrell, *Phys. Rev. B* **87**, 174428 (2010).
- ⁶J. P. van der Ziel, P. S. Persan, and L. D. Malmstrom, *Phys. Rev. Lett.* **15**, 190 (1965).
- ⁷A. H. M. Reid, A. V. Kimel, A. Kirilyuk, J. F. Gregg, and Th. Rasing, *Phys. Rev. Lett.* **105**, 107402 (2010).
- ⁸A. Kirilyuk, A. V. Kimel, and Th. Rasing, *Rev. Mod. Phys.* **82**, 2731 (2010).
- ⁹N. Kanda, T. Higuchi, H. Shimizu, K. Konishi, K. Yoshioka, and M. Kuwata-Gonokami, *Nat. Commun.* **2**, 1 (2011).
- ¹⁰J.-Y. Bigot, M. Vomir, and E. Beaupaire, *Nat. Phys.* **5**, 515 (2009).
- ¹¹Z. M. Jin, H. Ma, H. Wang, G. H. Ma, F. Y. Guo, and J. Z. Chen, *Appl. Phys. Lett.* **96**, 201108 (2010).
- ¹²Z. M. Jin, H. Ma, D. Li, G. H. Ma, M. Wang, and C. J. Zhao, *J. Appl. Phys.* **109**, 073109 (2011).
- ¹³G. H. Ma, D. Li, H. Ma, J. Ge, S. H. Hu, and N. Dai, *Appl. Phys. Lett.* **93**, 211101 (2008).
- ¹⁴M. Tonouchi, *Nat. Photonics* **1**, 97 (2007).
- ¹⁵B. Ferguson and X.-C. Zhang, *Nat. Mater.* **1**, 26 (2002).
- ¹⁶T. Dekorsy, W. Kutt, T. Pfeifer, and H. Kurz, *Europhys. Lett.* **23**, 223 (1993).
- ¹⁷A. P. Heberle, J. J. Baumber, and K. Kohler, *Phys. Rev. Lett.* **75**, 2598 (1995).
- ¹⁸T. Satoh, N. P. Duong, and M. Fiebig, *Phys. Rev. B* **74**, 012404 (2006).
- ¹⁹T. Kampfrath, A. Sell, G. Klatt, A. Pashkin, S. Mahrlein, T. Dekorsy, M. Wolf, M. Fiebig, A. Leitenstorfer, and R. Huber, *Nat. Photonics* **5**, 31 (2011).
- ²⁰K. Yamaguchi, M. Nakajima, and T. Suemoto, *Phys. Rev. Lett.* **105**, 237201 (2010).
- ²¹M. Nakajima, A. Namai, S. Ohkoshi, and T. Suemoto, *Opt. Exp.* **18**, 18260 (2010).
- ²²H. Luttgemeir, H. G. Bohn, and M. Brajczewska, *J. Magn. Magn. Mater.* **21**, 289 (1980).
- ²³D. Li, G. Ma, G. Ge, H. Su, and N. Dai, *Appl. Phys. B* **94**, 623 (2009).
- ²⁴G. V. Kozlov, S. P. Lebedev, A. A. Mukhin, A. S. Prokhorov, I. V. Fedorov, A. M. Balbashov, and L. Yu. Parsegllov, *IEEE Trans. Magn.* **29**, 3443 (1993).
- ²⁵I. Kezsmarki, N. Kida, H. Murakawa, S. Bordacs, Y. Onose, and Y. Tokura, *Phys. Rev. Lett.* **106**, 057403 (2011).
- ²⁶J. Kono, *Nat. Photonics* **5**, 5 (2011).